Journal of Inflammation Research

Dovepress
Taylor & Francis Group

Open Access Full Text Article

ORIGINAL RESEARCH

Supplementation of Glucosamine Selenium Ameliorates DSS-Induced Chronic Colitis in Mice via Affecting Gut Microbiota, Inhibiting Pyroptosis and Inactivating Chemokine Signaling Pathway

Tingting Zhao, Zhiyue Wen, Li Cui

Shanghai Key Laboratory of Veterinary Biotechnology, School of Agriculture and Biology, Shanghai Jiao Tong University, Shanghai, People's Republic of China

Correspondence: Li Cui, Shanghai Key Laboratory of Veterinary Biotechnology, School of Agriculture and Biology, Shanghai Jiao Tong University, 800 Dongchuan Road, Shanghai, 200240, People's Republic of China, Tel +86- 13918901989, Email lcui@sjtu.edu.cn

Introduction: Ulcerative colitis (UC) is a chronic disease that requires pharmacological therapy to achieve remission. This study aimed to evaluate the effect of glucosamine selenium (GASe) on chronic colitis and reveal the underlying regulatory mechanisms.

Methods: We evaluated the cumulative toxicity of GASe by gavage in mice for 40 days. Dextran sulfate sodium (DSS; 2.5%) was added to drinking water to induce chronic colitis, and GASe was administered to mice with chronic DSS colitis. 16S rRNA sequencing was performed to investigate the influence of GASe on gut microbiota, followed by diversity and LDA Effect Size (LEfSe) analyses. Differentially expressed genes (DEGs) associated with chronic DSS colitis were identified based on the expression profiling from the Gene Expression Omnibus (GEO) database and were subjected to functional enrichment analysis. Next, the effects of GASe on pyroptosis and chemokine signaling pathways were studied in vitro and in vivo.

Results: GASe had no significant toxicity in mice, and administration of low-GASe and high-GASe increased the length of the colon, inhibited the expression of IL-12, IL-6, and TNF-α, and improved colonic tissue structure. Low-GASe improved the diversity of the gut microbiota and mainly affected the *Burkholderiaceae* family, *Paenalcaligenes* genus, and *Erysipelatoclostridium* genus. Low-GASe and high-GASe suppressed the pyroptosis-related proteins NLRP3, GSDMD, and caspase-1. Furthermore, we identified 114 DEGs from the GSE87466 and GSE53306 datasets and these DEGs were mainly enriched in the chemokine signaling pathway and some inflammatory pathways. Further experiments showed that administration of GASe inhibited the chemokine signaling pathway in chronic DSS colitis mice and NCM460 cells.

Discussion: This study reveals abnormalities in the gut microbiota, pyroptosis, and chemokine signaling pathways involved in chronic colitis and may provide GASe as an alternative supplement for chronic colitis management.

Keywords: ulcerative colitis, glucosamine, selenium, 16S rRNA sequencing, differential expressed genes, chemokine

Introduction

Inflammatory bowel disease (IBD) is a chronic inflammatory disease and comprises Crohn's disease (CD), ulcerative colitis (UC), and indeterminate colitis[1]. The prevalence of IBD has been increasing in Western countries over the past decades, and a rapid increase in the incidence of IBD in Asian countries has recently been reported.[2] UC manifests as chronic inflammation and ulceration in the colon tissue. Patients with UC may present with bloody stools, fecal urgency, diarrhea, mucus, weight loss, abdominal pain, and asthenia.[3] Only 35% of patients with UC are likely to receive surgery[4] and, among patients with UC, operation-related complications are the leading cause of death.[5] Mesalazine, 5-aminosalicylic acid (5-ASA), is widely used for the remission or maintenance of remission in UC. Patients should receive systemic corticosteroids if remission is not induced, or even intravenous steroid injection if severe relapse occurs,[4] which may induce resistance to steroids. Therefore, it is necessary to develop novel therapies to relieve and treat UC.

Received: 12 July 2024
Accepted: 15 December 2024
Published: 12 March 2025

Glucosamine is a natural amino monosaccharide that exists in connective and cartilage tissues. Convincing evidence has shown that glucosamine is widely used as an effective and safe therapy to alleviate pain and functional impairments of osteoarthritis.[6] A previous study has demonstrated that N-palmitoyl-D-glucosamine attenuates 2,4-dinitrobenzene sulfonic acid-induced IBD through a PPAR-α-mediated regulatory mechanism.[7] In addition, a pre-clinical study has found that the combination of D-glucosamine and 5-ASA exerts inhibitory effects on inflammation and oxidation, thereby improving 2,4,6-trinitrobenzene sulfonic acid-induced colitis.[8] Selenium (Se) is an important element that serves as an active center of glutathione peroxidase and is involved in the oxidative response. Se supplementation has potential effects on the chronic inflammatory responses in IBD patients.[9,10] Huang reported that Se supplementation alleviates the symptomsof Crohn's disease and Th1 cell differentiation through selenoprotein W-mediated clearance of reactive oxygen species, indicating that Se is an essential T cell response regulator and a potential target for Crohn's disease treatment.[11] In addition, a recent clinical trial has demonstrated that Se supplementation can mitigate disease activity and improve the quality of life of patients with active mild-to-moderate UC.[12] Se-containing supplements, such as phycocyanin and Se nanoparticles, suppress UC by inactivating NF-κB.[13,14] Glucosamine selenium (GASe) is a new form of selenium that remarkably increases the diversity of the gut microbiota of *Penaeus vannamei*.[15] However, little is known about the effects of GASe on chronic colitis or its potential mechanisms.

Pyroptosis is a pro-inflammatory programmed cell death mediated by inflammasome and gasdermin proteins.[16] Pyroptosis is crucial for host defense against pathogenic infections during normal physiological processes, whereas abnormal pyroptosis triggers immoderate and continuous inflammatory responses, which may lead to inflammatory diseases.[17] Gasdermin-E-regulated pyroptosis is implicated in the pathogenesis of Crohn's disease by enhancing intestinal inflammation.[18] Activation of PPAR-γ-TLR4-NF-κB signaling pathway and suppression of gasdermin-D-mediated pyroptosis in macrophages may be associated with the inhibitory effect of honokiol on UC.[19] Notably, a recent study has found that Se nanoparticles improve intestinal health by regulating the pyroptosis-related NLRP3 signaling pathway.[20] Meanwhile, Se-enriched black soybean reducesbenzo[a]pyrene-induced toxicity in the colon through the gut microbiota.[21] It has been speculated that the effect of Se supplementation on colonic injury may be associated with pyroptosis; however, further research is warranted.

In this study, we identified differentially expressed genes (DEGs) associated with dextran sulfate sodium (DSS)-induced chronic colitis and found these DEGs were enriched in the chemokine signaling pathway. Chemokines and chemokine receptors are crucial regulators of the intestinal mucosal homeostasis. Recently, Liu et al demonstrated that CXCL8 plays a vital role in the pathophysiological mechanism of UC, and targeting the CXCL8-CXCR1/2 axis represents a promising method for UC treatment.[22] In addition, blocking CCL2 suppresses chronic colitis-related carcinogenic effects in mice.[23] However, whether GASe inhibits chemokine signaling pathways remains unclear. Hence, we focused on the chemokine signaling pathway and investigated the effects of GASe on this pathway in a DSS-induced colitis mouse model and DSS-induced NCM460 cells.

Methods

Animals

A total of 80 male C57BL/6 mice (6–8 weeks old, 18–20 g) were obtained from SiPeiFu Biotechnology Co., Ltd (Beijing, China) and kept at 22 ± 2°C under controlled humidity (50–60% humidity) with a 12 h light/dark cycle. Animals had free access to standard food and water. The experiments were performed in compliance with the guidelines of laboratory animal care and approved by the Local Ethics Committee.

DSS-Induced Colitis Mouse Model

Thirty mice were randomly divided into three groups: control group, 2.5% DSS group, and 3% DSS group (n = 10 per group). To induce chronic colitis, DSS was dissolved in drinking water at concentrations of 2.5% (2.5% DSS group) and 3% (3% DSS group) and administered to mice for 40 days. Mice in the control group received normal drinking water. The body weight of the mice was recorded daily. Body weight loss was assessed using the following scores: 0, < 1%; 1, 1–5%; 2, 5–10%; 3, 10–15%; and 4, > 15%. The presence or absence of blood in the feces was determined based on 0, negative; 2,

hidden blood in the stool; and 4, bloody stool. Stool characteristics were evaluated based on the following scores: 0, negative; 2, loose stools; and 4, diarrhea.[24] On day 40, the mice were anesthetized, and eyeball blood samples were collected. Mice were sacrificed by cervical dislocation, and colon tissues were harvested and stored at –80°C until use.

Preparation of GASe

GASe was prepared by Jiangsu Shuanglin Marine Biological Pharmaceutical Co., Ltd (lot number: 20200702, Jiangsu, China). The molecular formula of GASe is $(C_{10}H_{14}O_{10}N_2)Se$ (molecular weight: 401).

Safety Evaluation of GASe

Twenty mice were assigned to four groups: control group, low-GASe group (50 mg/kg), moderate-GASe group (100 mg/kg), and high-GASe group (200 mg/kg) (n = 5 per group). To evaluate the safety of GASe, 0.1 mL of GASe at concentrations of 50, 100, and 200 mg/kg was administered daily by gavage to the mice for 40 days. Mice in the control group were administered by gavage 0.1 mL PBS for 40 days. At 12 h after the final administration, the mice were anesthetized and eyeball blood samples were collected. Mice were sacrificed, and the heart, liver, spleen, lung, kidney, and colon tissues were collected and weighed. The organ index was calculated using the following formula: organ weight/body weight × 100%. The length of colon tissue was measured and then stored at –80°C.

GASe Treatment

To study the effect of GASe on chronic DSS colitis, 24 mice were administered with 2.5% DSS in drinking water for 5 days and then switched to normal drinking water for 7 days, and mice were treated in this way until the end of the 40 day experiment. Mice in the control group consumed water throughout the entire process. On day 29, DSS mice were divided into the chronic DSS colitis group, positive control group (150 mg/kg, 5-aminosalicylic acid (5-ASA)), low-GASe group (100 mg/kg), and high-GASe group (200 mg/kg) (n = 6 for each group). Fecal samples were collected for sequencing over the last 2 days. On day 40, blood samples were collected under anesthesia, and part of the colon tissue was collected for pathological examination. The remaining tissue was stored at –80°C.

Hematoxylin-Eosin (H&E) Staining

Pathological changes in the colon tissues of mice with chronic DSS colitis were evaluated using H&E staining. Colon tissues of mice were fixed with 4% paraformaldehyde (Solarbio, China) overnight and then dehydrated using ascending concentrations of ethanol (50%, 70%, 80%, 90%, 95%, and 100%). Next, the tissues were embedded in paraffin and cut into 4-μm slides. After dewaxing with xylene and rehydration with ethanol, slides were stained with hematoxylin (H9627, Sigma-Aldrich USA) for 5 min and 0.5% eosin (E4009, Sigma-Aldrich USA) for 1 min. Pathological changes were examined under a microscope (Nikon, Tokyo, Japan).

Quantitative Reverse-Transcription Polymerase Chain Reaction (qRT-PCR)

Total RNA was extracted from colon tissues using TRIZOL reagent (Invitrogen, USA). The concentration of extracted RNAs (5 μL) was measured at 260 nm and 280 nm using a UV spectrophotometer, and RNAs with the ratio of OD260/OD280 at 1.9–2.0 were selected for further analysis. Subsequently, first-strand cDNA was synthesized using Hiscript II QRT Supermix for qPCR kits (Vazyme, China). qRT-PCR program was conducted using the ChamQ Universal SYBR kit (Vazyme, China) on ABI7500 system (Applied Biosystems) under the thermocycler conditions: initial denaturation at 95°C for 30 s, 40 cycles of denaturation at 95°C for 10 s and annealing at 60°C for 30 s. GAPDH was used as the housekeeping gene. The relative expression was calculated using the $2^{-\Delta\Delta CT}$ method.[25] The primer sequences used for qRT-PCR are listed in Table 1. Three independent experiments were performed for each gene.

ELISA Assays

To determine the serum levels of proinflammatory cytokines, serum samples were obtained from blood samples after centrifugation at 4000 rpm for 10 min at 4°C. For ELISA assays in NCM460 cells, the cellular supernatant was collected and then centrifuged for 20 min at 4°C. The levels of serum IL-12, IL-6, TNF-α, IL-18, IL-1β, and lactate dehydrogenase

Table 1 The Primers Sequences for qRT-PCR

Gene Names	Sense	Antisense
GAPDH	AACTTTGGCATTGTGGAAGG	ACACATTGGGGGTAGGAACA
IL-6	TACCCCCAGGAGAAGATTCC	TTTTCTGCCAGTGCCTCTTT
IL-10	TGGTGAAACCCCGTCTCTAC	CTGGAGTACAGGGGCATGAT
TNF-α	ACGGAGAAGAAGCAGACCAA	CGCAGTTCAAAGGTCTCCTC
MUC2	CAAGATCTTCATGGGGAGGA	AACACGGTGGTCCTCTTGTC
TJP1	TGAGGCAGCTCACATAATGC	GGTCTCTGCTGGCTTGTTTC

(LDH) were measured using ELISA kits, according to the manufacturer's instructions (Esebio Biotechnology Co., Ltd, China). Absorbance (OD value) was measured at 450 nm using a microplate reader (Thermo Fisher USA).

Western Blotting

Total proteins were extracted from mice and NCM460 cells after DSS or GASe treatment using a radioimmunoprecipitation assay (RIPA) buffer (Biosharp, China), and their concentrations were determined using a Pierce BCA kit. Proteins were separated by 10% sodium dodecyl sulfate-polyacrylamide gel electrophoresis (SDS-PAGE), transferred onto polyvinylidene fluoride (PVDF) membranes for 60 min, and blocked with 5% non-fat milk for 2 h. The Primary rabbit monoclonal antibodies against ZO-1 (1:1000, ab307799), occludin (1:1000, ab216327), claudin-1 (1:2000, ab211737), NLRP3 (1:1000, ab263899), GSDMD (1:1000, ab219800), caspase-1 (1 μg/mL, ab138483), CXCL1 (1:100, ab206411), and CXCL2 (1:1000, ab275879) were incubated with membranes at 4°C overnight. HRP-labeled secondary antibodies (1:2000, ab205718) were used for 1 h at room temperature. GAPDH was used as an internal control. The ECL luminescence reagent was used for color development on a Tanon 5200 system. The ImageJ software was used to calculate the gray values of the protein bands.

Analysis of Gut Microbiota

To analyze changes in the gut microbiota, 200 mg fecal samples were used for microbial DNA extraction using a TIANamp Bacteria DNA Kit (TianGen Biochemical Technology Co., LTD, Beijing, China). The V3–V4 variable regions of the 16S rRNA genes were amplified using TransStart Fastpfu DNA Polymerase (TransGen AP221-02). Amplified products were extracted, purified, and sequenced on an Illumina MiSeq platform (Illumina, USA). For alpha diversity (within-habitat diversity), QIIME dada2 was used to calculate Chao1 (community richness), Shannon (community diversity), Simpson, observed species, Faith_pd, Pielou_e, and Goods_coverage. Rank abundance and operational taxonomic unit (OTU) rank curves were constructed to reflect the richness and diversity of the gut microbiota. Beta diversity (between-habitat diversity) analysis was conducted to evaluate the composition and distribution of gut microbiota. Furthermore, principal coordinate analysis (PCoA) was used to study the similarities or differences in microbial community composition. PERMANOVA and ANOSIM analyses were performed to analyze the statistical differences in microbial community composition between the control and treatment groups. In addition, a petal diagram was generated to determine the common and specific microbial species among different samples. The differences in the abundance of the microbial community were analyzed using the LDA Effect Size (LEfSe) with a threshold of 2. The R software was used to analyze the species composition of the metabolic pathways based on the stratified sample metabolic pathway abundance.

Identification of Differential Expressed Genes (DEGs) and Functional Enrichment Analysis

The expression profiles of patients with UC were downloaded from the GSE87466 and GSE53306 datasets in the Gene Expression Omnibus (GEO, https://www.ncbi.nlm.nih.gov/geo/) database by searching for "ulcerative colitis." The GSE87466 dataset comprised 87 UC and 21 normal mucosal biopsy samples, while the GSE53306 dataset included 40 single endoscopic pinch biopsies. The data were normalized, and an overview of the data distribution was evaluated using boxplots. GEO2R (https://www.ncbi.nlm.nih.gov/geo/geo2r/) was used to identify DEGs between healthy samples

and UC samples with p <0.05, and |log2FoldChange| ≥1.5 (UC). DEGs were visualized using volcano plots and their expression patterns were displayed in a heatmap. The co-DEGs at the intersection of the DEGs between the GSE87466 and GSE53306 datasets were visualized using a Venn diagram (http://www.ehbio.com/test/venn/#/). To understand biological functions, Kyoto Encyclopedia of Genes and Genomes (KEGG) functional enrichment analysis was performed using DAVID (https://david.ncifcrf.gov/summary.jsp).

Preparation of Drug-Containing Serum (GASe-DS)

To prepare GASe-DS, two male SD rats were administrated by gavage with 1 mL/100 g GASe (200 mg/kg) twice daily for 3 days. One hour after the last administration, the rats were euthanized using carbon dioxide suffocation and blood samples were collected from the abdominal aorta. Serum samples were obtained by centrifugation at 2500 rpm for 10 min and then inactivated at 56°C for 30 min. Next, the serum samples were filtered using 0.22 μm microporous membrane filters to eliminate bacteria. The collected GASe-DS was stored at –80°C until use.

Cell Culture

NCM460, normal human colon mucosal epithelial cells, were obtained from icell Bioscience Inc. (Shanghai, China) and cultured in DMEM medium (HyClone, USA) containing 10% FBS (Biosera, France), 1% streptomycin-penicillin (Beyotime Institute of Biotechnology) at 37°C in an incubator with 95% humidity and 5% CO_2. Cells were grouped into control, DSS, DSS + GASe-DS, DSS + GASe-DS + TFA, and DSS + GASe-DS + reparixin groups. To induce chronic colitis in NCM460 cells, 2% DSS (MP Biomedicals, USA) was added to the cellular medium and incubated for 24 h when the cells reached 70–80% confluence.[26] ATI-2341 TFA (TFA, 0.2umol/kg), the chemokine pathway agonist, was used in DSS + GASe-DS cells to evaluate the effect of GASe on the chemokine pathway. To verify the effect of GASe on the chemokine pathway, the chemokine pathway antagonist reparixin (1 μM, Med-ChemExpress) was added to the DSS + GASe-DS cells.

Cell Viability Measurement

After treatment with DSS, GASe-DS and GASe-DS + Reparixin, cells were seeded into 96-well plates (1×10^4 cells/well) and incubated for 24 h. According to the manufactures' instructions, 10 μL of CCK-8 solution (Beyotime, China) and 90 μL medium were added to each well, and cells were incubated at 37°C for 2 h. The absorbance was determined at 450 nm using a microplate reader (Thermo Fisher Scientific, USA).

Cell Apoptosis

Apoptotic cells were assessed using the Annexin V-FITC/propidium iodide (PI) Apoptosis Detection Kit (Vazyme, China). After treatment, NCM460 cells (3×10^5cells/well) were seeded into 6-well plates and stained with FITC-labeled Annexin V (5 μL) and PI (5 μL). Cells were incubated in the dark at room temperature for 15 min. Apoptotic cells were counted using a flow cytometer (Beckman Coulter) and the rate of cell apoptosis was analyzed using FlowJo software.

Statistical Analysis

All experimental data were analyzed using GraphPad Prism 9.0 (GraphPad Prism Software Inc., San Diego, CA, USA) and the values are presented as the mean ± SD of duplicate assays. One-way analysis of variance (ANOVA) was used for comparisons among multiple groups, followed by Tukey's multiple comparison test. *T*-tests were used to compare two groups. Statistical significance was determined when the p value was lower than 0.05.

Results

DSS-Induced Chronic Colitis Mouse Model

To establish a mouse model of chronic colitis, mice were administered with 2.5% or 3% DSS for 40 days. As shown in Figure 1A, the administration of 2.5% DSS or 3% DSS significantly reduced the body weight of mice compared to that in the control group ($p < 0.001$). In addition, we measured the colon length of the mice. Compared to the control group, the colon length of the DSS-treated mice was significantly decreased ($p < 0.001$) (Figure 1B and C). Pathological

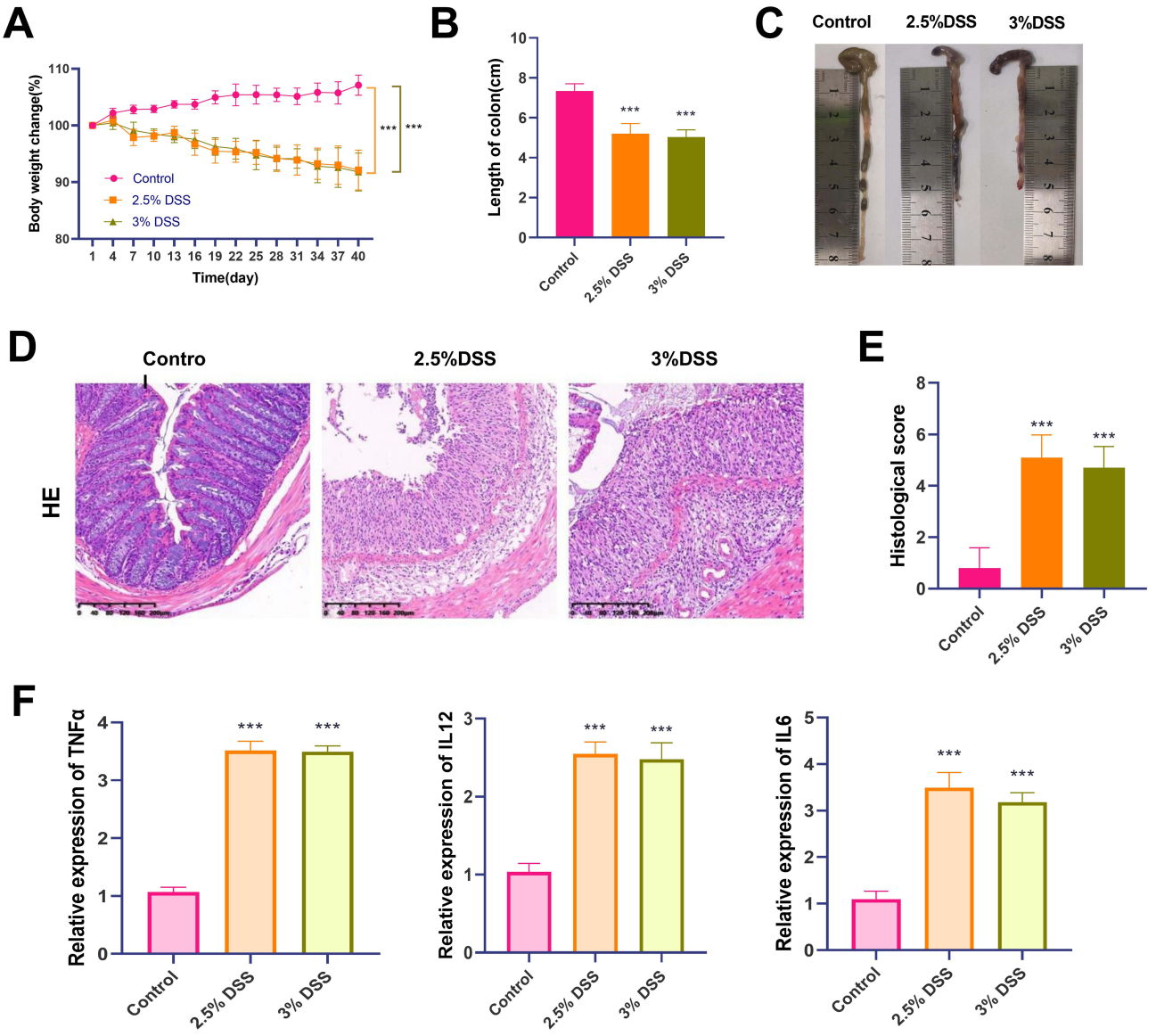

Figure 1 Induction of UC mouse model by administration of DSS. (**A**) Administration of 2.5% DSS or 3% DSS induces reductions in body weight of mice. (**B** and **C**) Pictures of colon tissues and histogram of colon length. The colon length of chronic DSS colitis mice is significantly decreased. (**D**) H&E staining shows destroyed colon tissue structure and inflammatory cells infiltration in chronic DSS colitis mice (magnification 100×; scale bar 200 μm). (**E**) Chronic DSS colitis mice exhibit a higher histological score. (**F**) Increased release of pro-inflammatory cytokines TNF-α, IL-12, and IL-6 in chronic DSS colitis mice. *** $p < 0.001$, compared with the control group.

examination by H&E staining revealed that the colon tissue structure of control mice was clear and was rich in tightly arranged goblet cells without infiltration of inflammatory cells, while administration of DSS significantly changed the colon tissue structure, disrupted colon tissue structure, and promoted the infiltration of a large number of inflammatory cells (Figure 1D). Mice treated with 2.5% DSS or 3% DSS exhibited higher histological scores than the control group ($p < 0.001$) (Figure 1E). The levels of pro-inflammatory cytokines TNF-α, IL-12, and IL-6 were remarkably elevated in the 2.5% DSS and 3% DSS groups compared with those in the control group ($p < 0.001$) (Figure 1F).

Accumulative Toxicity Evaluation of GASe

Elemental analysis of GASe was performed by scanning electron microscope, and the results showed that there were elements including C (41.49%), N (8.73%), O (15.98%), and Se (33.80%) (Figure S1). The time-of-flight secondary ion mass spectrometry analysis found that cluster aggregation phenomenon occurred in GASe (Figure S2). X-ray

photoelectron spectroscopy displayed that GASe was mainly composed of negatively divalent and a small amount of zero valent selenium elements (Figure S3).

The cumulative toxicity of GASe was evaluated in normal mice, and there was no visible alteration in the activity and mental state of mice after 40 days of GASe administration by gavage. The body weight of mice in the control or GASe-treated groups (low-GASe, moderate-GASe, and high-GASe) gradually increased within 40 days (Figure 2A). Administration of low-GASe, moderate-GASe, and high-GASe did not significantly alter the colon length ($p > 0.05$) (Figure 2B). There were no significant differences in the organ indices of the heart, liver, spleen, lung, and kidney tissues in low-GASe, moderate-GASe, and high-GASe groups compared with the control group ($p > 0.05$) (Figure 2C). No statistically significant differences in TbiL and ALT levels were observed in low-GASe, moderate-GASe, and high-GASe mice compared with the control group ($p > 0.05$) (Figure 2D). Low-GASe, moderate-GASe, and high-GASe administration had no significant effects on the classification and proportion of leukocytes when compared with the control group ($p > 0.05$) (Figure 2E). Long-term GASe treatment did not alter the white blood cell, red blood cell, and hemoglobin counts ($p > 0.05$) (Figure 2F).

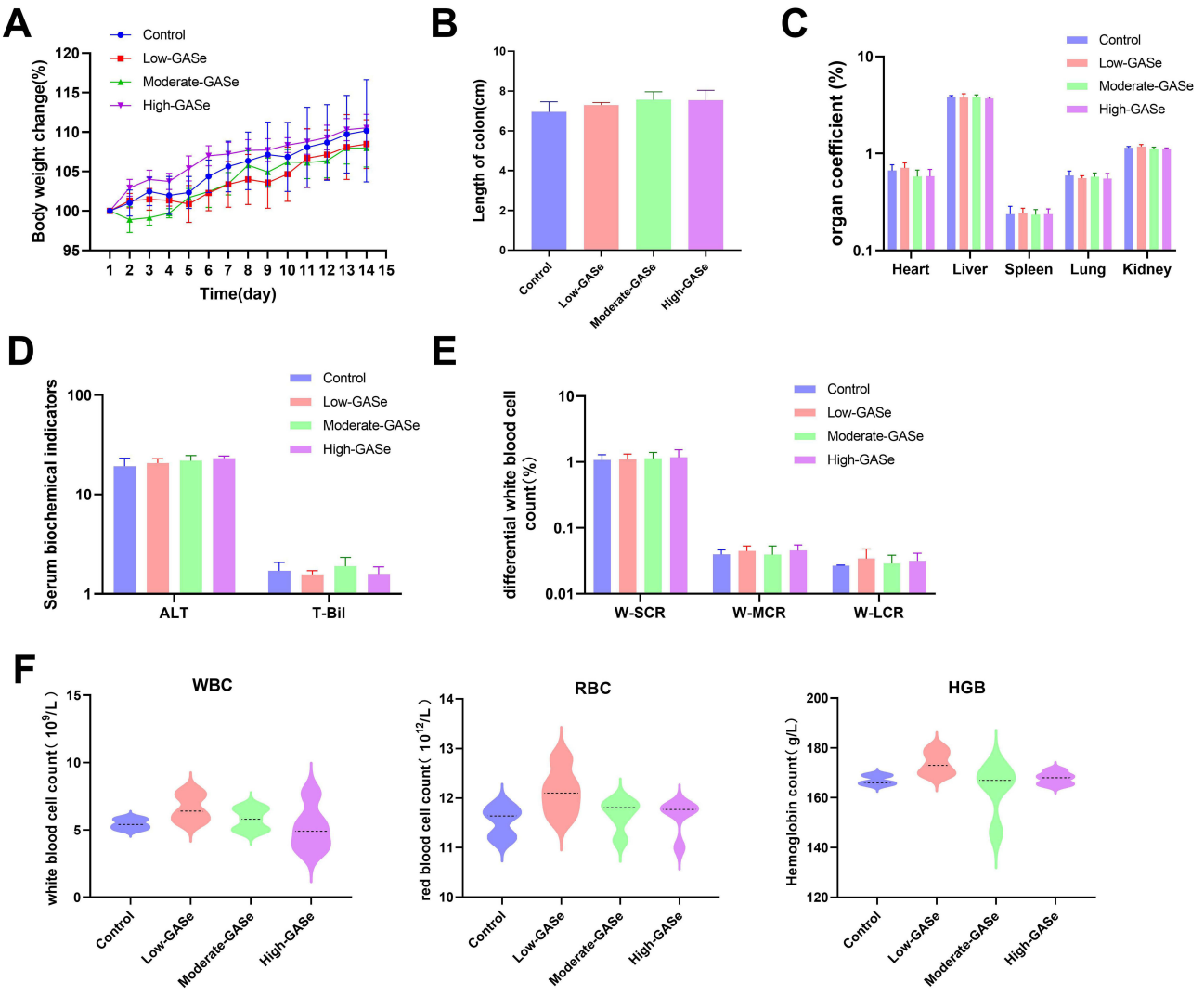

Figure 2 Accumulative toxicity evaluation of GASe. (**A**) Changes of body weight of mice after GASe administration for 40 days. (**B**) No significant changes in the length of colon after GASe administration. (**C**) No significant difference in the organ index of heart, liver, spleen, lung, and kidney tissues in the GASe-treated groups. (**D**) Serum biochemical index ALT and Tbil contents after GASe administration. (**E**) Changes in the classification and proportion of leukocytes in the GASe-treated groups. (**F**) The counting of white blood cells, red blood cells, and hemoglobin.

https://doi.org/10.2147/JIR.S486751

Administration of GASe Ameliorates Chronic DSS Colitis

Figure 3A displays the experimental flow chart. Within 7 days of DSS administration, the body weight of mice was significantly reduced, while the mice showed increased tolerance to DSS; on the 40th day, the body weight of the control ($p < 0.001$), low-GASe ($p < 0.001$) and high-GASe ($p < 0.001$) mice had notably increased compared with the chronic DSS colitis mice (Figure 3B). The colon length of mice in the positive control group was significantly increased ($p < 0.01$), and the colon length in the low-GASe mice ($p < 0.05$) and high-GASe mice ($p < 0.01$) was significantly longer than that in the chronic DSS colitis mice (Figure 3C). Administration of low-GASe and high-GASe effectively inhibited the release of IL-12, IL-6, and TNF-α ($p < 0.01$) compared with chronic DSS colitis (Figure 3D). The colonic crypt

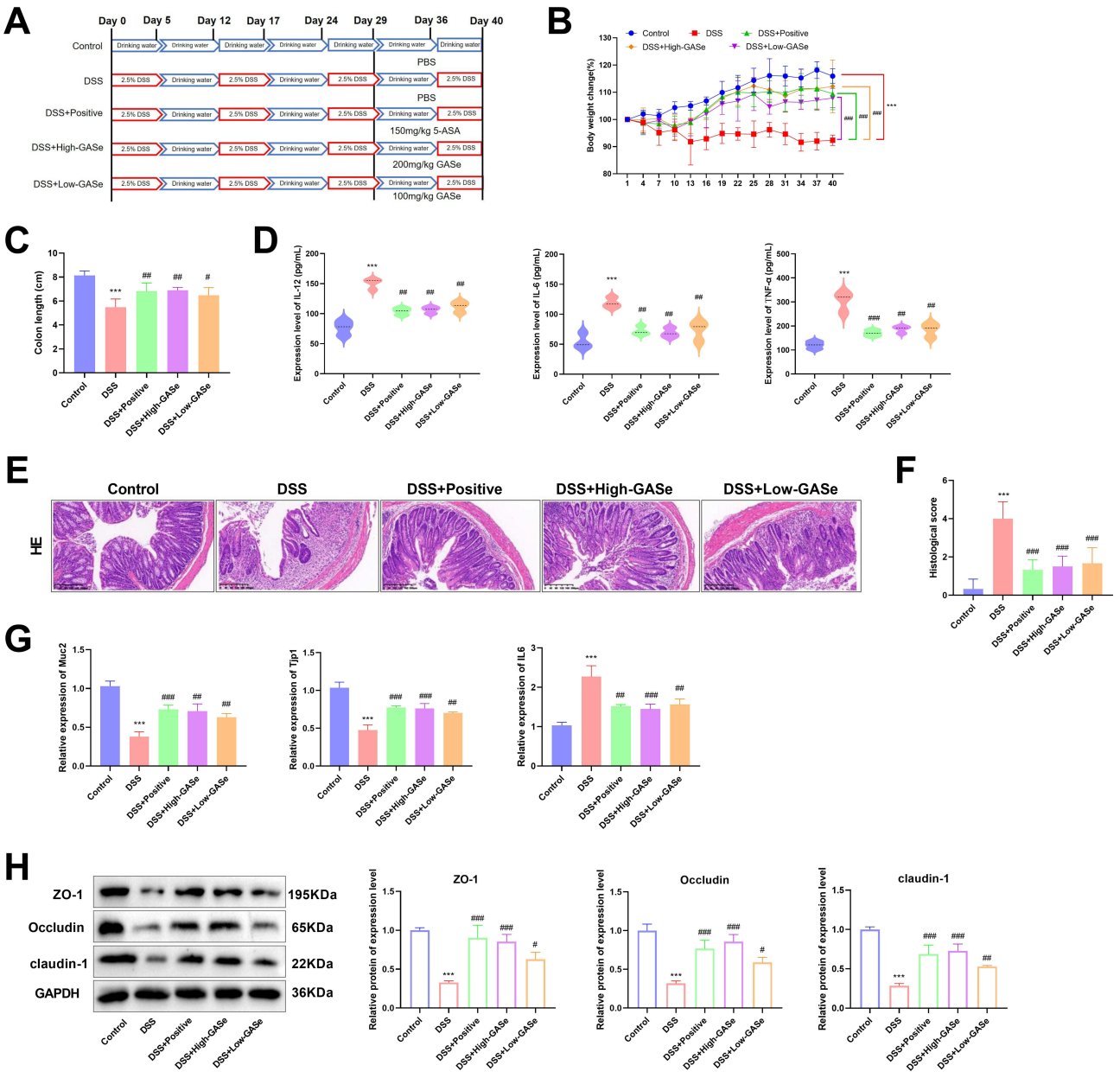

Figure 3 Administration of GASe ameliorates chronic colitis in mice. (**A**) The 40-day experimental flow chart. (**B**) Changes of the body weight of control, positive control, and GASe treatment groups. (**C**) Histogram of colon length after GASe treatment. (**D**) GASe treatment effectively inhibits the release of IL-12, IL-6, and TNF-α. (**E**) H&E staining shows the recovery of colon tissue structure and decreased inflammatory cells infiltration after GASe treatment (magnification 100×; scale bar 200 μm). (**F**) Alteration of histological score after GASe treatment. (**G**) GASe administration promotes the production of Muc2 and Tjp1, but inhibits the release of IL-6. (**H**) Western blot analysis shows increased expression of ZO-1, Occludin and claudin-1 in GASe groups. *** $p < 0.001$, compared with the control group. $^{\#}p < 0.05$, $^{\#\#}p < 0.01$ and $^{\#\#\#}p < 0.001$, compared with the chronic DSS colitis group.

https://doi.org/10.2147/JIR.S486751

organization and mucosal upper layer of control mice were intact, without inflammatory cell infiltration or congestion, whereas the colon tissue of mice with chronic DSS colitis exhibited severe pathological changes, accompanied by branching, distortion, swelling, and disappearance of crypts. The thickness of the crypt base was increased, and severe inflammatory cells and congestion were observed; the positive control treatment alleviated colonic lesions, with intact crypt structure, less branching, twisting, and reduced congestion, but with a small amount of inflammatory cell infiltration. High-GASe restored intact crypt structures, but there was a small amount of congestion and inflammatory cell infiltration, whereas low-GASe alleviated chronic colitis, but the crypt structure was damaged, with distortion and inflammatory cell infiltration (Figure 3E). DSS dramatically increased the histological score compared with the control group ($p < 0.001$), while the application of low-GASe and high-GASe remarkably decreased the histological score compared with the DSS group ($p < 0.001$) (Figure 3F). Figure 3G shows that the positive control treatment, low-GASe and high-GASe administration promoted the production of Muc2 and Tjp1 ($p < 0.01$ or $p < 0.001$) but inhibited the release of IL-6 ($p < 0.01$ or $p < 0.001$) compared with the chronic DSS colitis group. Western blot analysis showed that the positive control treatment, low-GASe and high-GASe administration significantly enhanced the expression of ZO-1, Occludin, and claudin-1 compared with the DSS group ($p < 0.001$ or $p < 0.05$) (Figure 3H).

GASe Affects the Gut Microbiota of Chronic DSS Colitis Mice

We evaluated alpha diversity within the habitat, or intra-community diversity, to reflect the changes in richness and evenness of the gut microbiota. Mice in the control group had the highest alpha diversity index, such as Chao1, Observed species, Shannon, Faith_pd, and Pielou_e, as well as the lowest Goods_coverage, whereas mice in DSS group and treatment group exhibited decreased alpha diversity. High-GASe and positive treatment had significantly lower Chao1, Observed species, Shannon, Faith_pd, and Pielou_e compared with the control group ($p < 0.01$ or $p < 0.05$), while low-GASe increased the alpha diversity index (Figure 4A). The rank abundance curve shows the homogeneity and richness of samples. As shown in Figure 4B, mice in the control group had the highest homogeneity and richness of gut microbiota, and the administration of low-GASe reversed the decreased homogeneity and richness in chronic DSS colitis mice. The OTU rank curve revealed that high-GASe mice had the fastest curve decline, suggesting that mice in the high-GASe group had the lowest diversity of gut microbiota (Figure 4C). Moreover, we evaluated beta diversity, which was related to differences in the composition and distribution of gut microbiota. The results from PcoA showed a distinct separation between the control group and the other groups, implying significant differences in species composition between the control group and the other groups (Figure 4D). Statistically significant differences were observed between the control and low-GASe groups ($p < 0.05$) (Figure 4E).

Alterations of Species of Gut Microbiota

To determine the common and specific microbial species among different samples, petal diagrams were generated, and 344 common species were identified: samples in the control group had 7884 species, followed by 4506 species in the low-GASe group and 3817 species in the chronic DSS colitis group; samples in the high-GASe group had the fewest species (2850) (Figure 5A). LEfSe analysis revealed that the main specific species in the control group were *Muribaculaceae* family and *Muribaculum* genus; *Tannerellaceae* and *Parabacteroides* genera were the main specific species in the chronic DSS colitis group; *Deferribacteres* phylum was specific to the positive control group; *Burkholderiaceae* family, *Paenalcaligenes* genus, and *Erysipelatoclostridium* were predominant in the low-GASe group; and high-GASe mice had an increased abundance of *Streptococcus* genus (Figure 5B). Through metabolic pathway analysis, we found that *Muribaculum* was the main genus that contributed to metabolism in the control group, *Bacteroides* and *Alistipes* were the major contributors to metabolism in the chronic DSS colitis group and other treatment groups (Figure 5C).

GASe Suppresses Pyroptosis in Chronic DSS Colitis Mice

To evaluate the effect of GASe on pyroptosis in chronic DSS colitis, we measured the expression of IL-1β, IL-18, and LDH. Compared to the control group, the production of IL-1β, IL-18, and LDH was remarkably enhanced in the chronic DSS colitis group ($p < 0.001$); administration of low-GASe and high-GASe significantly inhibited the release of IL-1β

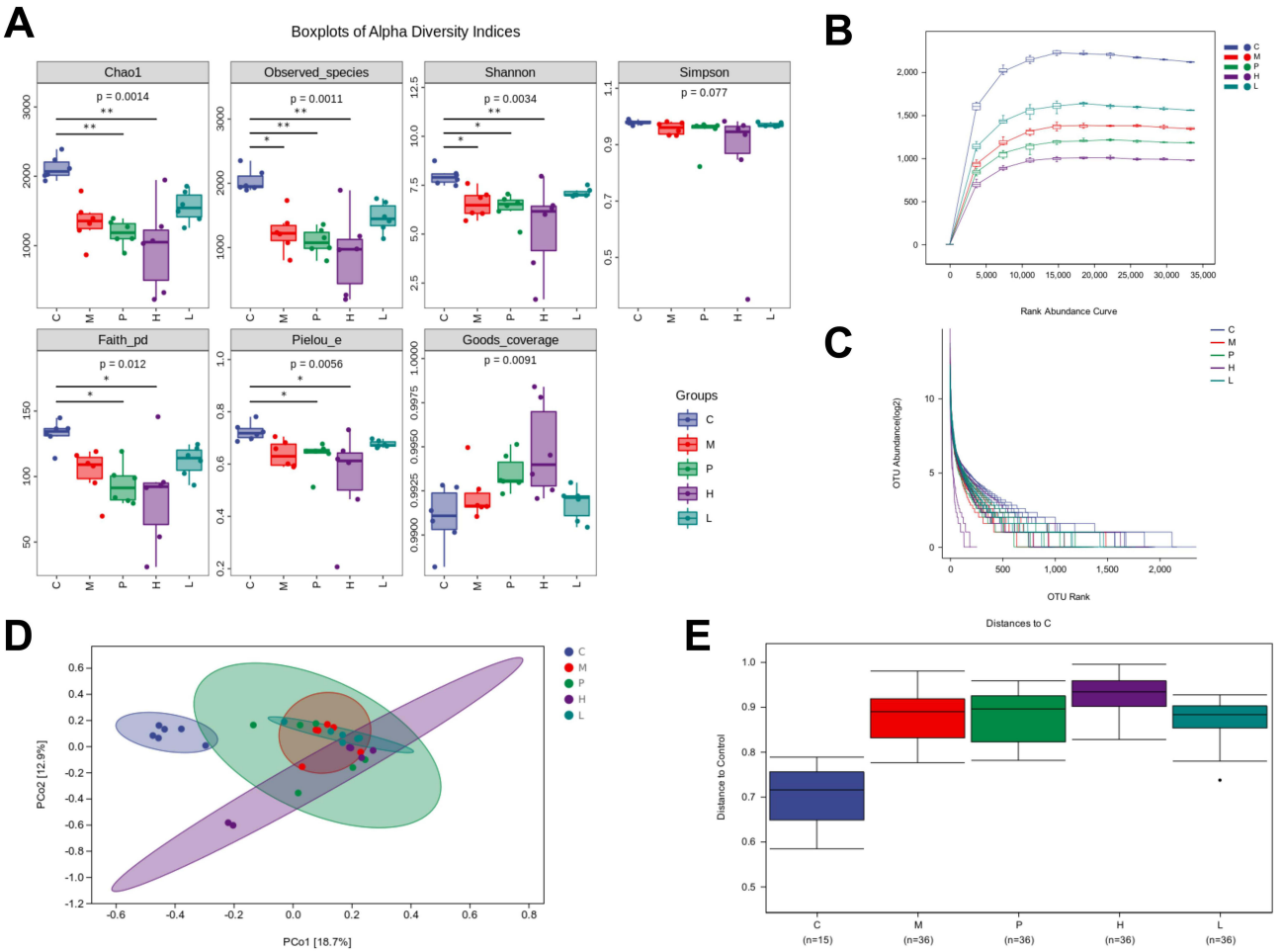

Figure 4 GASe alters the gut microbiota of chronic DSS colitis mice. (**A**) Changes of alpha diversity index such as Chao1, Observed species, Shannon, Simpson, Faith_pd, Pielou_e, and Goods_coverage. (**B**) The rank abundance curves show the homogeneity and richness of the samples. (**C**) The OTU rank curves of samples. (**D**) PCoA shows distinct separation between control group and other groups. (**E**) Statistically difference between the control group and low-GASe group based on PERMANOVA and anosim. C, control group, M, model group (chronic DSS colitis), P, positive control group, L, low-GSAe, H, high-GSAe group. *$p < 0.05$ and **$p < 0.01$ compared with control group.

($p < 0.01$ or $p < 0.05$), IL-18 ($p < 0.001$), and LDH ($p < 0.01$) compared with DSS group (Figure 6A). Moreover, DSS significantly promoted the expression of pyroptosis-related proteins, such as NLRP3, GSDMD, and caspase-1, compared with the control group ($p < 0.001$), whereas administration of low-GASe and high-GASe considerably downregulated the expression of NLRP3 ($p < 0.001$), GSDMD ($p < 0.001$ or $p < 0.01$), and caspase-1 ($p < 0.001$) (Figure 6B).

GASe Regulates Chemokine Signaling Pathway

Identification of DEGs and Functional Enrichment Analysis

Differential expression analysis was performed to identify DEGs in the GSE87466 and GSE53306 datasets. We identified 633 DEGs in the GSE87466 dataset and 376 DEGs in the GSE53306 dataset ($p < 0.05$ and $|\log2FoldChange| \geq 1.5$) (Figure 7A). Data from 48 samples in the GSE87466 dataset and 29 samples in the GSE53306 dataset were normalized, and their distribution is displayed in Figure S4A. The results indicated that the normalized data were aligned. The top 15 upregulated and 15 downregulated genes were clustered using a heat map, which showed good sample clustering (Figure S4B). A total of 114 co-DEGs were identified at the intersection of the GSE87466 and GSE53306 datasets (Figure 7B). Furthermore, 114 co-DEGs were subjected to KEGG enrichment analysis. These DEGs were mainly enriched in the IL-17 signaling pathway, cytokine and cytokine receptor interaction, TNF signaling pathway, and chemokine signaling pathway (Figure 7C and D).

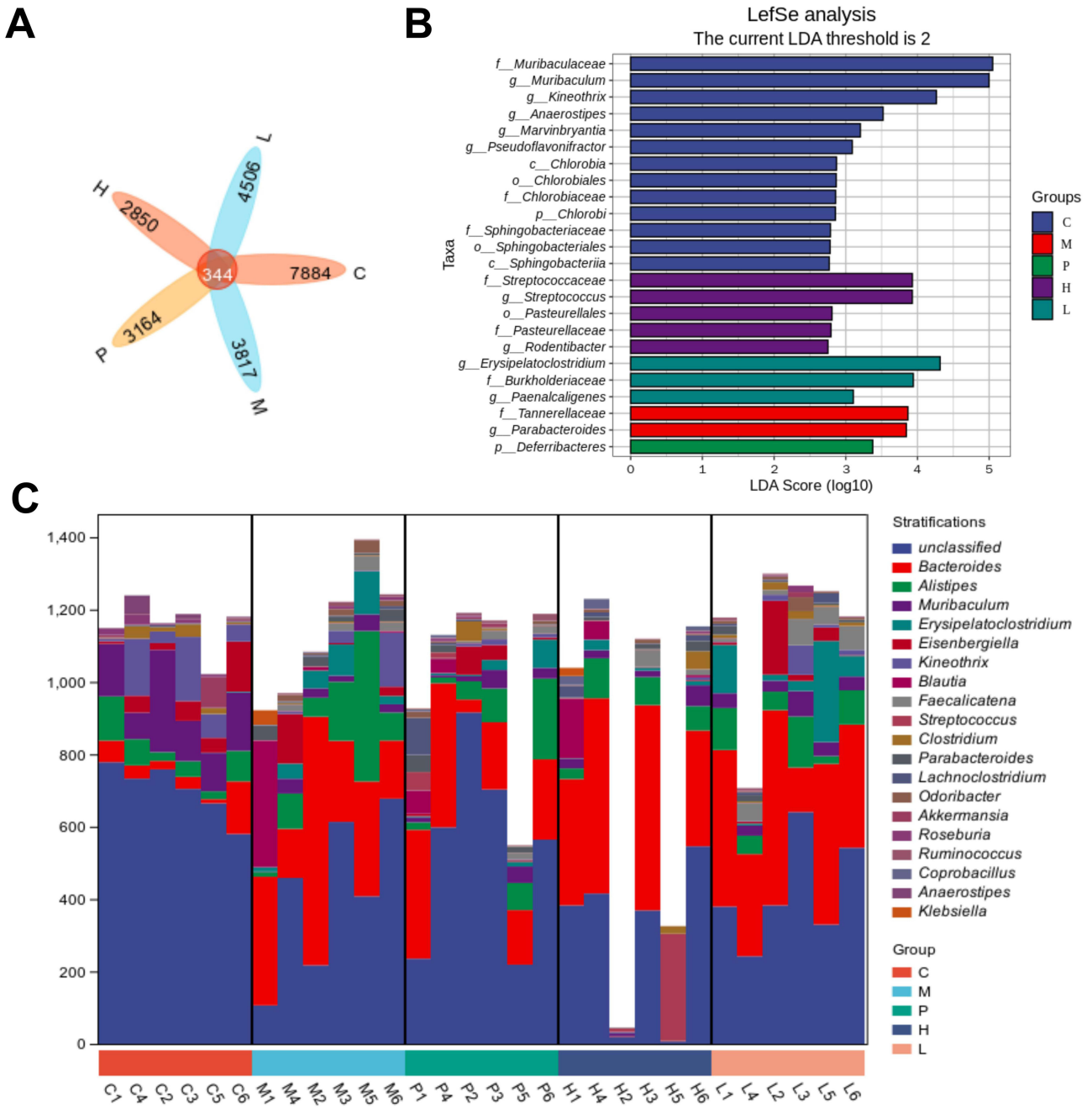

Figure 5 Difference analysis of species of gut microbiota. (**A**) Petal diagram reveals the common species and specific microbial species among different treatment groups. (**B**) LEfSe analysis of specific species in different treatment groups. (**C**) Alteration of specific microbial species composition of metabolic pathways in different treatment groups. Horizontal coordinates represent groups and vertical coordinates represent the relative abundance of metabolic pathways. C, control group, M, model group (chronic DSS colitis), P, positive control group, L, low-GSAe, H, high-GSAe group.

GASe Inhibits Chemokine Signaling Pathway in Chronic DSS Colitis Mice

Next, we measured the expression levels of chemokine signaling pathway-related proteins using Western blot analysis. The expression of CXCL1 and CXCL2 was significantly higher in DSS group than that of the control group ($p < 0.001$), whereas administration of high-GASe or low-GASe notably repressed the expression of CXCL1 and CXCL2 compared to that in the chronic DSS colitis group ($p < 0.001$ or $p < 0.01$) (Figure 7E).

https://doi.org/10.2147/JIR.S486751

https://doi.org/10.2147/JIR.S486751

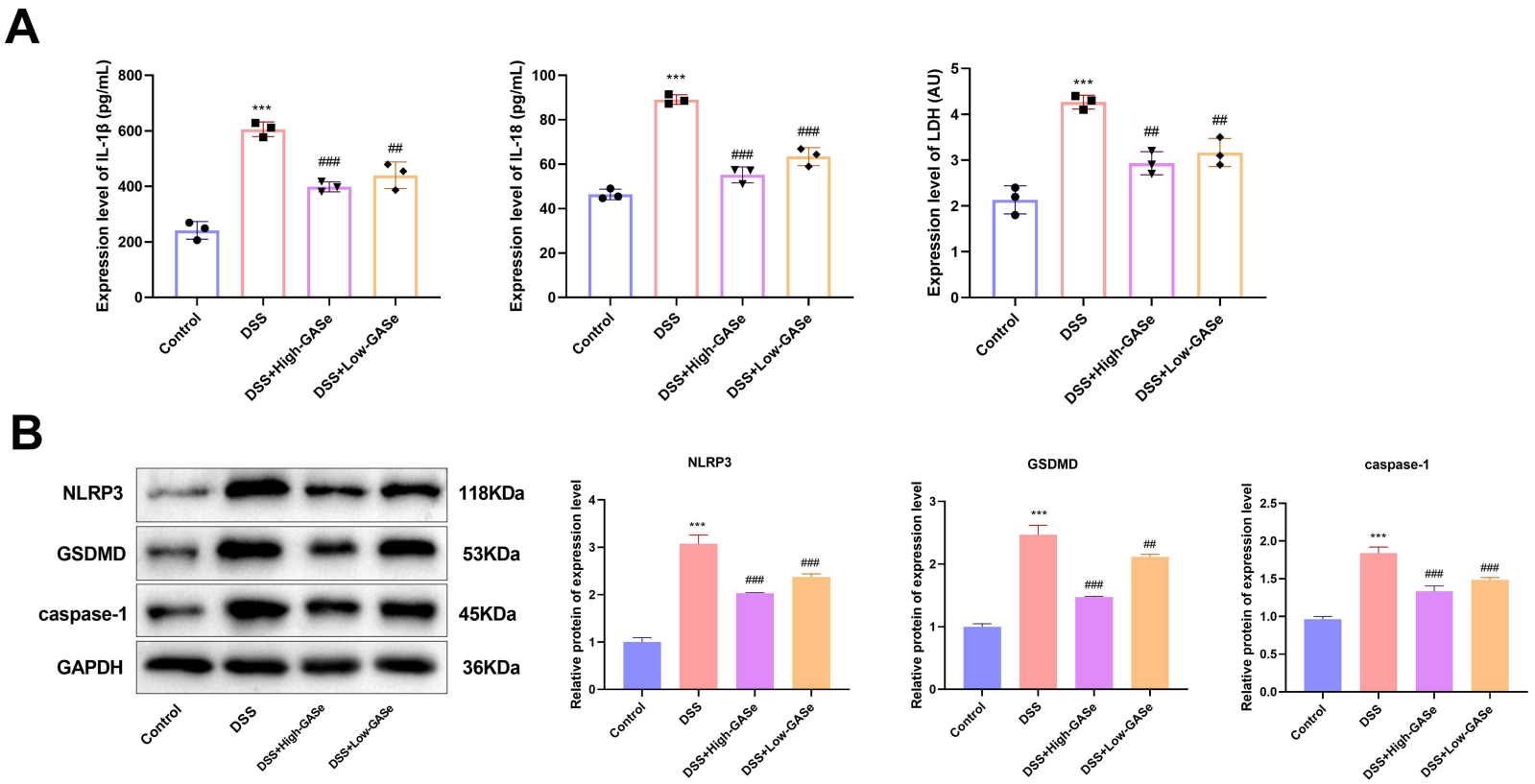

Figure 6 GASe suppresses pyroptosis in chronic DSS colitis mice. (**A**) Administration of GASe reduces the expression levels of IL-1β, IL-18, and LDH measured by ELISA. (**B**) Administration of GASe inhibits the expression of pyroptosis-related proteins NLRP3, GSDMD and caspase-1. $^{***}p < 0.001$, compared with the control group. $^{\#\#}p < 0.01$ and $^{\#\#\#}p < 0.001$, compared with the chronic DSS colitis group.

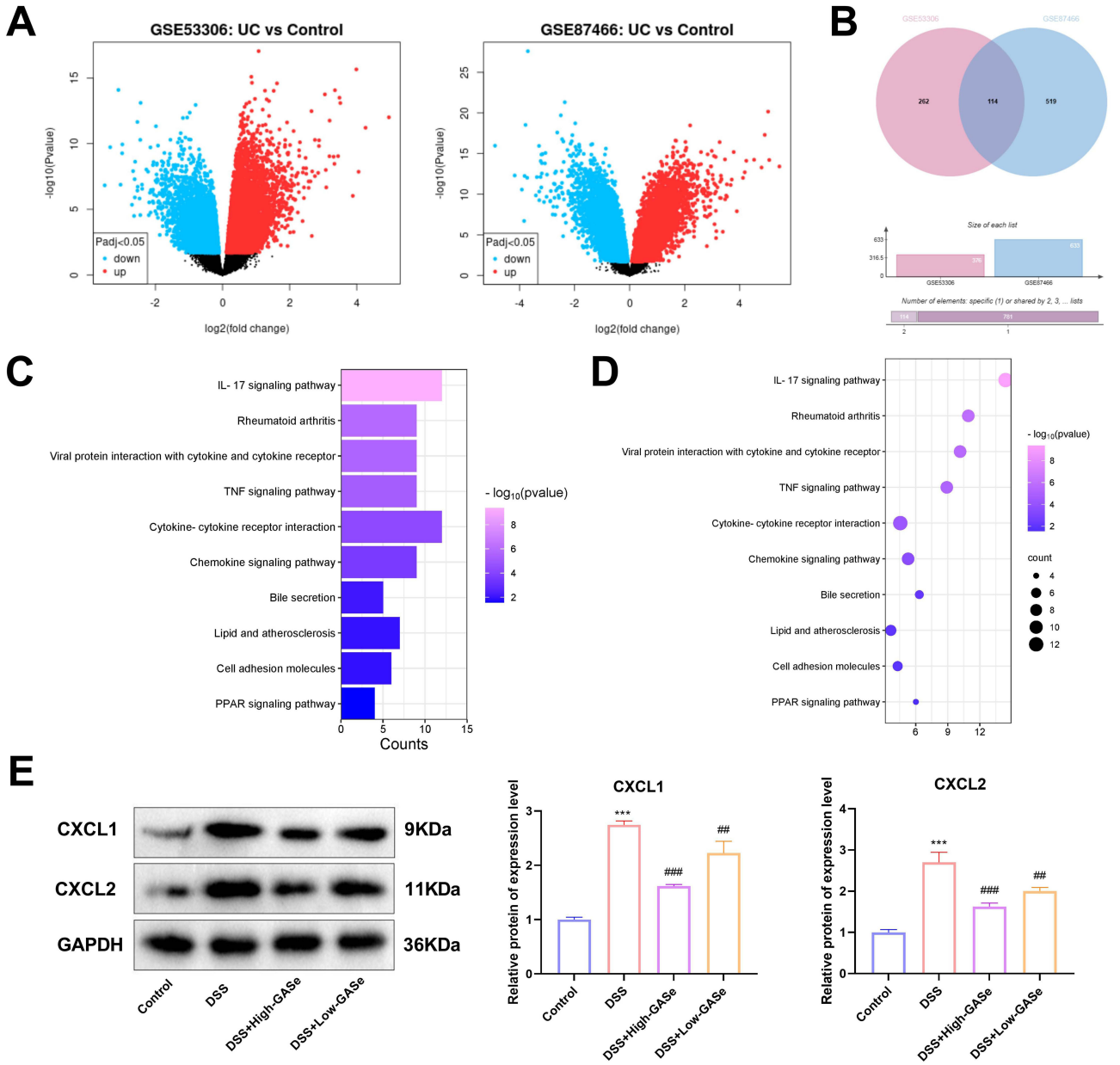

Figure 7 GASe affects chemokine signaling pathway. (**A**) Volcano plots show upregulated and downregulated DEGs in the GSE87466 dataset and GSE53306 dataset. Red plots represent upregulated genes and blue ones represent downregulated genes. (**B**) A total of 114 co-DEGs at the intersection of GSE87466 and GSE53306 datasets. (**C** and **D**) KEGG enrichment analysis for 114 co-DEGs. (**E**) Western blot analysis reveals GASe inhibits the expression of CXCL1 and CXCL2 in chronic DSS colitis mice. ***$p < 0.001$, compared with the control group. ##$p < 0.01$ and ###$p < 0.001$, compared with the DSS group.

GASe-DS Ameliorates DSS-Induced Inflammatory Response via Inactivating Chemokine Signaling Pathway

As shown in Figure 8A, 10% GASe-DS induced a significant reduction in cell viability, whereas 1% GASe-DS was not significantly toxic to cells. Therefore, we selected 1% GASe-DS for analysis. The cell viability of NCM460 cells treated with DSS was significantly decreased compared with the control group ($p < 0.001$), while GASe-DS abolished the inhibitory effect of DSS on cell viability ($p < 0.05$). Application of TFA considerably decreased cell viability compared with DSS + GASe-DS cells ($p < 0.001$), whereas the chemokine pathway antagonist reparixin remarkably enhanced cell viability compared with DSS + GASe-DS cells ($p < 0.05$) (Figure 8B). Meanwhile, administration of GASe-DS notably suppressed cell apoptosis in DSS-treated NCM460 cells compared with the DSS group ($p < 0.001$), while TFA

https://doi.org/10.2147/JIR.S486751

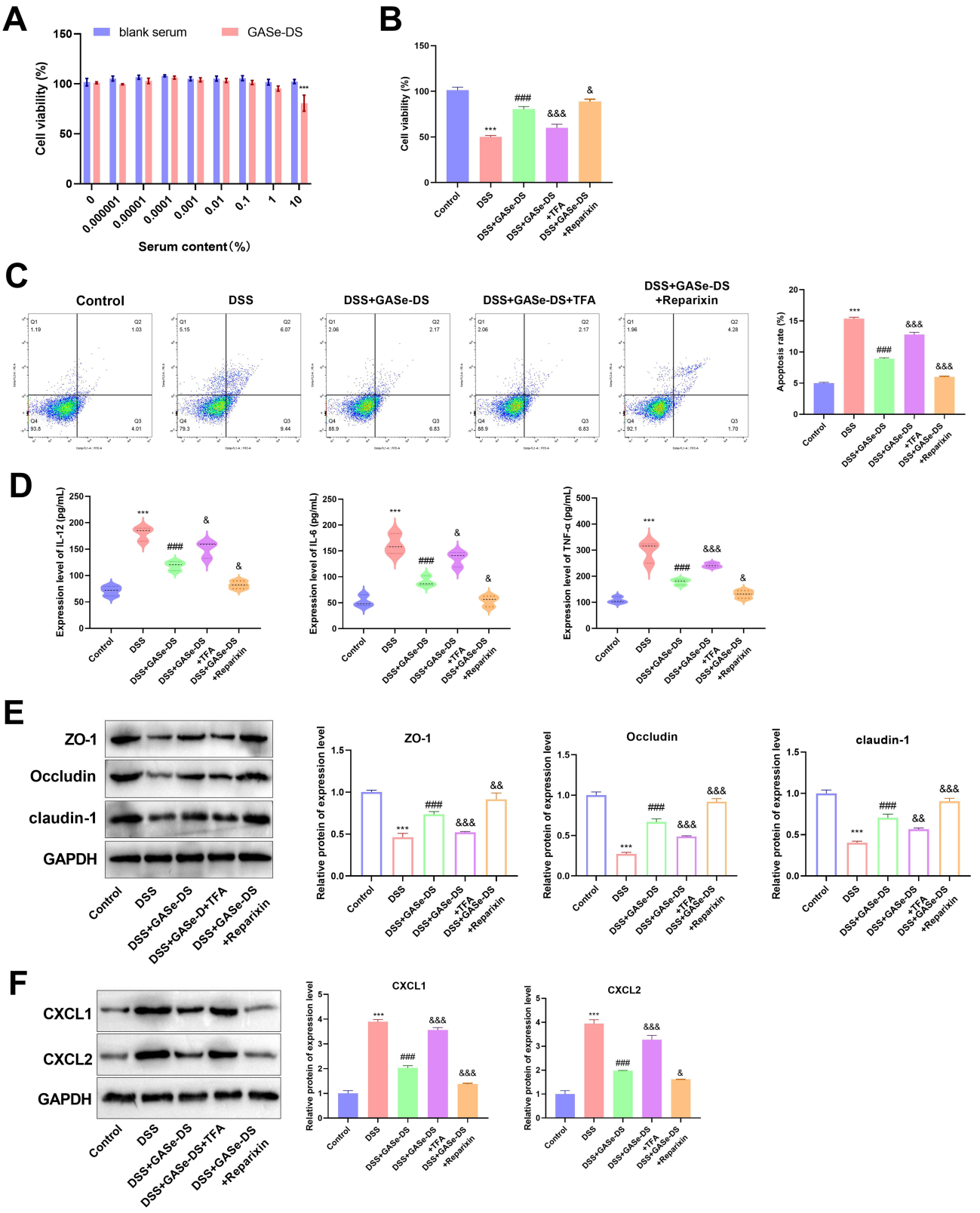

Figure 8 GASe-DS alleviates DSS-induced cell apoptosis and inflammatory response via inactivating chemokine signaling pathway. (**A**) The effects of series of GASe-DS content on cell viability. (**B**) 1% GASe-DS and reparixin increase cell viability, while ATI-2341 TFA decreases cell viability of DSS-treated NCM460 cells. (**C**) Flow cytometry shows that GASe-DS and reparixin treatment decrease cell apoptosis, while ATI-2341 TFA increases cell apoptosis. (**D**) Administration of GASe-DS and reparixin decrease the levels of IL-12, IL-6 and TNF-α. ATI-2341 TFA promotes the expression of IL-10, IL-6 and TNF-α. (**E**) Western blot analysis reveals that administration of GASe-DS and reparixin promote the expression of ZO-1, Occludin and claudin-1, and ATI-2341 TFA downregulates ZO-1, Occludin and claudin-1 in NCM460 cells. (**F**) Administration of GASe-DS and reparixin downregulate the expression of CXCL1 and CXCL2, which is reversed by ATI-2341 TFA in NCM460 cells. $^{***}p < 0.001$, compared with the control group. $^{\#\#\#}p < 0.001$, compared with the DSS group. $^{\&}p < 0.05$, $^{\&\&}p < 0.01$, and $^{\&\&\&}p < 0.001$, compared with the DSS + GASe-DS group.

 https://doi.org/10.2147/JIR.S486751

significantly increased cell apoptosis compared with DSS + GASe-DS cells ($p < 0.001$). Further reparixin application notably decreased the apoptotic rate compared with DSS + GASe-DS cells ($p < 0.001$). (Figure 8C). The results of ELISA showed that DSS significantly induced the production of IL-10, IL-6, and TNF-α compared to the control group ($p < 0.001$), whereas administration of GASe-DS considerably downregulated the production of IL-10, IL-6, and TNF-α compared to the DSS group ($p < 0.001$). Application of TFA significantly promoted the production of IL-10 ($p < 0.05$), IL-6 ($p < 0.05$), and TNF-α ($p < 0.001$) compared with DSS + GASe-DS group, whereas reparixin dramatically decreased the levels of IL-12, IL-6, and TNF-α compared with DSS + GASe-DS group ($p < 0.05$) (Figure 8D).

Additionally, we found that the expression of the tight junction proteins ZO-1, Occludin, and claudin-1 was downregulated in DSS-treated NCM460 cells compared with control cells ($p < 0.001$), while administration of GASe-DS upregulated their expression compared with DSS-treated cells ($p < 0.001$). Administration of TFA exerted the inhibitory effects on ZO-1 ($p < 0.001$), Occludin ($p < 0.001$), and claudin-1 ($p < 0.001$) compared with DSS + GASe-DS, however, the effects of TFA on ZO-1 ($p < 0.01$), Occludin ($p < 0.001$), and claudin-1 ($p < 0.001$) were reversed by reparixin (Figure 8E). The effects of DSS on the expression of CXCL1 and CXCL2 were repressed by GASe-DS ($p < 0.001$). Application of TFA significantly upregulated the expression of CXCL1 and CXCL2 compared with DSS + GASe-DS group ($p < 0.001$), whereas the expression of CXCL1 ($p < 0.001$) and CXCL2 ($p < 0.05$) was dramatically suppressed by reparixin (Figure 8F).

Discussion

Ulcerative colitis (UC) is a chronic disease associated with an inflammatory response and dysbiosis of the gut microbiota. Nutrient supplementation may be beneficial for patients with UC who require long-term medication. Therefore, we focused on a new form of Se-containing glucosamine and investigated its role in chronic DSS colitis.

In this study, we evaluated the cumulative toxicity of GASe by oral gavage for 40 days. We found that GASe had no physical or mental toxicity to mice, and the administration of GASe could increase colon length. This finding suggested that GASe administration had no significant cumulative toxicity. We successfully established a chronic DSS colitis model using 2.5% and 3% DSS. Administration of low-GASe and high-GASe inhibited the release of inflammatory cytokines and improved colonic tissue structure, demonstrating that GASe could effectively alleviate chronic DSS colitis. We discovered that low-GASe increased the diversity of the gut microbiota in chronic DSS colitis and identified *Erysipelatoclostridium* as the predominant genus in the low-GASe group. The results indicated that low-GASe alleviated chronic DSS colitis by altering the diversity of the gut microbiota and mainly affecting the *Burkholderiaceae* family, *Paenalcaligenes* genus, and *Erysipelatoclostridium* genus. Moreover, GASe ameliorated chronic DSS colitis by suppressing pyroptosis and chemokine signaling pathways.

Dysbiosis of gut microbiota plays a pivotal role in the development of chronic colitis. *Tannerellaceae* is oral pathogenic bacteria that contribute to the inflammatory response. Application of DSS promotes an increase in the abundance of *Parasutterella, Burkholderiales,* and *Tannerellaceae*, whereas administration of probiotic consortia decreases the abundance ofmicrobiota in DSS-induced colitis,[27] thus contributing to the improvement of IBD symptoms. Consistent with a previous study, in an IBD mouse model induced by 5-day DSS administration, the abundance of *Tannerellaceae* decreases from day 3 to day 7, and the relative abundance of *Tannerellaceae* is positively correlated with the loss of body weight in IBD mice.[28] In the present study, LEfSe discovered that the *Tannerellaceae* family was the main specific species in chronic DSS colitis mice, which suggests that DSS induced chronic colitis mainly by increasing the abundance of the *Tannerellaceae* family. This discrepancy may be due to the timing of DSS administration and changes in the inflammatory response. In addition, Liu et al have found few *Burkholderiaceae* in normal mice, while they find a decreased abundance of *Burkholderiaceae* in colitis mice accompanied by sleep fragmentation and increased *Burkholderiaceae* after electroacupuncture.[29] *Erysipelatoclostridium*, a butyrate-producing bacterium, as well as *Alistipes*, is abundant after barley leaf insoluble dietary fiber supplementation, which exerts inhibitory effects on DSS-induced inflammation.[30] In addition, Deng has noticed that cisplatin increases the abundance of *Erysipelatoclostridium, Aeromonas*, and *Staphylococcus* but decreases the abundance of *Alistipes*, whereas Se-containing albumin nanoparticles attenuate cisplatin-induced intestinal mucositis by increasing *Bacteroidetes, Firmicutes, Clostridia*, and *Erysipelotrichi*.[31] The discrepancy in *Erysipelatoclostridium* between our study and Deng's results may be due to the different models and treatments. A meta-analysis has demonstrated decreased abundance of *Bacteroides* is related to the development of IBD.[32] In this study, we

found that administration of low-GASe significantly increased the abundance of the *Burkholderiaceae* family, *Paenalcaligenes* genus, and *Erysipelatoclostridium* genus. The findings indicated that the increased abundance of the *Burkholderiaceae* family, *Paenalcaligenes* genus, and *Erysipelatoclostridium* genus was associated with the anti-inflammatory effects of GASe. Additionally, we found that *Bacteroides* and *Alistipes* were the major contributors to metabolism in the treatment groups. These results might imply that alteration of *Bacteroides* and *Alistipes* after low-GASe administration attenuate chronic DSS colitis by affecting the metabolism.

In human visceral adipose tissue, Nguyen-Ngo C has demonstrated that pretreatment with Se reduces the release of lipopolysaccharide (LPS)-stimulated pro-inflammatory cytokines and the expression of CCL chemokines (CCL2 and CCL8) and CXCL chemokines (CXCL1, CXCL2, CXCL5, CXCL8, and CXCL10).[33] Additionally, administration of Se inhibits LPS-induced expression of pro-inflammatory cytokines, including IL-1A, IL-1B, and IL-6, as well as chemokines, such as CXCL1, CXCL5, and CXCL8.[34] These findings collectively decipher the inhibitory effects of Se on the chemokine pathways. Recently, Se-containing compounds have been widely developed as therapeutic agents, owing to their antioxidative and anti-inflammatory effect.[35] In the current study, bioinformatic analytical methods were used to identify DEGs that might contribute to the pathogenesis of chronic DSS colitis and revealed that these DEGs were mainly enriched in the chemokine signaling pathway and some inflammatory pathways (IL-17 signaling pathway, cytokine and cytokine receptor interaction, and TNF signaling pathway). Furthermore, we showed that administration of GASe ameliorated DSS-induced pyroptosis, inflammatory cytokines such as IL-12, IL-6, TNF-α, IL-1β, and IL-18, and chemokine signaling pathway-related proteins (CXCL1 and CXCL2). Therefore, this study demonstrates for the first time that Se-containing glucosamine may regulate pyroptosis and chemokine signaling pathways in chronic DSS colitis.

Although we have demonstrated the role of GASe in alleviating chronic DSS colitis, this study has some limitations. First, UC is a chronic disease, and patients with UC and severe disease may experience relapse. Thus, the safety of the long-term use of GASe should be evaluated using experimental studies or clinical trials. Moreover, the administration of GASe to patients with different severities of illness should be investigated in future studies. Second, LEfSe analysis revealed the main specific species after GASe treatment, and there is currently a lack of correlation analysis between the gut microbiota and inflammatory indicators, chemokines, or chemokine receptors to screen for key species associated with inflammation and chemokine pathways. Furthermore, the identified DEGs warrant further functional studies to identify biomarkers related to chronic colitis.

Conclusion

In conclusion, this study demonstrates that GASe may be a safe and effective method for chronic colitis management. Additionally, administration of low-GASe can improve the diversity of the gut microbiota in mice with chronic DSS colitis, mainly affecting the *Erysipelatoclostridium* genus. Application of GASe attenuates chronic DSS colitis by suppressing pyroptosis and inactivating the chemokine signaling pathway. These results suggest that GASe may be a potential therapeutic option for chronic colitis.

Data Sharing Statement

The datasets used and/or analyzed during the current study are available from the corresponding author upon reasonable request.

Ethical Approval

Compliance with the National Institutes of Health Guidelines for the Care and Use of Laboratory Animals approved by the Animal Ethics Committee of the Shanghai Key Laboratory of Veterinary Biotechnology, School of Agriculture and Biology, Shanghai Jiao Tong University. (No. WTPZ20231021001). The publicly available data used in this study was downloaded from the public databases and it would not have had any effect on patient outcomes. This study was declared exempt from the ethical statement according to the ethics approval statement of our ethics committee.

Author Contributions

All authors made a significant contribution to the work reported, whether in the conception, study design, execution, acquisition of data, analysis, and interpretation, or in all these areas, took part in drafting, revising, or critically reviewing the article; gave final approval of the version to be published; have agreed on the journal to which the article has been submitted; and agree to be accountable for all aspects of the work.

Funding

Shanghai Science and Technology Commission science and technology innovation project experimental animal special; No: 21140901400. Additional support was provided by the same project under Grant No. 23141900100.

Disclosure

The authors declare that they have no conflicts of interest in this work.

References

1. Saez A, Herrero-Fernandez B, Gomez-Bris R, Sánchez-Martinez H, Gonzalez-Granado JM. Pathophysiology of inflammatory bowel disease: innate immune system. *Int J mol Sci*. 2023;24(2):1526. doi:10.3390/ijms24021526
2. Mak WY, Zhao M, Ng SC, Burisch J. The epidemiology of inflammatory bowel disease: east meets west. *J Gastroenterol Hepatol*. 2020;35(3):380–389. doi:10.1111/jgh.14872
3. Nóbrega VG, Silva I, Brito BS, Silva J, Silva M, Santana GO. The onset of clinical manifestations in inflammatory bowel disease patients. *Arquivos de gastroenterologia*. 2018;55:290–295. doi:10.1590/s0004-2803.201800000-73
4. Wehkamp J, Götz M, Herrlinger K, Steurer W, Stange EF. Inflammatory bowel disease: crohn's disease and ulcerative colitis. *Dtsch Arztebl Int*. 2016;113(5):72. doi:10.3238/arztebl.2016.0072
5. Burisch J, Munkholm P. The epidemiology of inflammatory bowel disease. *Scand J Gastroenterol*. 2015;50(8):942–951. doi:10.3109/00365521.2015.1014407
6. Vo NX, Le NNH, Chu TDP, et al. Effectiveness and safety of glucosamine in osteoarthritis: a systematic review. *Pharmacy*. 2023;11(4):117. doi:10.3390/pharmacy11040117
7. Palenca I, Seguella L, Del Re A, et al. N-Palmitoyl-D-glucosamine inhibits TLR-4/NLRP3 and improves DNBS-induced colon inflammation through a PPAR-α-dependent mechanism. *Biomolecules*. 2022;12(8):1163. doi:10.3390/biom12081163
8. Roy S, Dhaneshwar S, Mahmood T, Kumar S, Saxena SK. Pre-clinical investigation of protective effect of nutraceutical D-glucosamine on TNBS-induced colitis. *Immuno Immunotoxicol*. 2023;45(2):172–184. doi:10.1080/08923973.2022.2128370
9. Nettleford SK, Prabhu KS. Selenium and selenoproteins in gut inflammation—a review. *Antioxidants*. 2018;7(3):36. doi:10.3390/antiox7030036
10. Zhong Y, Jin Y, Zhang Q, et al. Comparison of selenium-enriched lactobacillus paracasei, selenium-enriched yeast, and selenite for the alleviation of DSS-induced colitis in mice. *Nutrients*. 2022;14(12):2433. doi:10.3390/nu14122433
11. Huang L-J, Mao X-T, Li Y-Y, et al. Multiomics analyses reveal a critical role of selenium in controlling T cell differentiation in crohn's disease. *Immunity*. 2021;54(8):1728–1744.e1727. doi:10.1016/j.immuni.2021.07.004
12. Khazdouz M, Daryani NE, Cheraghpour M, et al. The effect of selenium supplementation on disease activity and immune-inflammatory biomarkers in patients with mild-to-moderate ulcerative colitis: a randomized, double-blind, placebo-controlled clinical trial. *Eur J Nutr*. 2023;62:1–10.
13. Zhu C, Zhang S, Song C, et al. Selenium nanoparticles decorated with Ulva Lactuca polysaccharide potentially attenuate colitis by inhibiting NF-κB mediated hyper inflammation. *J Nanobiotechnol*. 2017;15(1):1–15. doi:10.1186/s12951-017-0252-y
14. Zhu C, Ling Q, Cai Z, et al. Selenium-containing phycocyanin from Se-enriched Spirulina platensis reduces inflammation in dextran sulfate sodium-induced colitis by inhibiting NF-κB activation. *Journal of Agricultural and Food Chemistry*. 2016;64(24):5060–5070. doi:10.1021/acs.jafc.6b01308
15. Meng-qi L, Wen-can H, Jian-an S, Xiang-zhao M. Effect of glucosamine selenium on growth, quality and intestinal microflora of Penaeus vannamei. *Feed Res*. 2022;45(9).
16. Yu P, Zhang X, Liu N, Tang L, Peng C, Chen X. Pyroptosis: mechanisms and diseases. *Signal Transduct Target Ther*. 2021;6(1):128. doi:10.1038/s41392-021-00507-5
17. Rao Z, Zhu Y, Yang P, et al. Pyroptosis in inflammatory diseases and cancer. *Theranostics*. 2022;12(9):4310. doi:10.7150/thno.71086
18. Tan G, Huang C, Chen J, Chen B, Zhi F. Gasdermin-E-mediated pyroptosis participates in the pathogenesis of Crohn's disease by promoting intestinal inflammation. *Cell Rep*. 2021;35(11):109265. doi:10.1016/j.celrep.2021.109265
19. Wang N, Kong R, Han W, et al. Honokiol alleviates ulcerative colitis by targeting PPAR-γ–TLR4–NF-κB signaling and suppressing gasdermin-D-mediated pyroptosis in vivo and in vitro. *Int Immunopharmacol*. 2022;111:109058. doi:10.1016/j.intimp.2022.109058
20. Chen Y, Wu W, Zhou H, et al. Selenium nanoparticles improved intestinal health through modulation of the NLRP3 signaling pathway. *Frontiers in Nutrition*. 2022;9:907386. doi:10.3389/fnut.2022.907386
21. Wang Z, Shi L, Li H, Song W, Li J, Yuan L. Selenium-Enriched Black Soybean Protein Prevents Benzo (a) pyrene-Induced Pyroptotic Colon Damage and Gut Dysbacteriosis. *J Agric Food Chem*. 2022;70(39):12629–12640. doi:10.1021/acs.jafc.2c04526
22. Zhu Y, Yang S, Zhao N, et al. CXCL8 chemokine in ulcerative colitis. *Biomed Pharmacother*. 2021;138:111427. doi:10.1016/j.biopha.2021.111427
23. Popivanova BK, Kostadinova FI, Furuichi K, et al. Blockade of a chemokine, CCL2, reduces chronic colitis-associated carcinogenesis in mice. *Cancer Res*. 2009;69(19):7884–7892. doi:10.1158/0008-5472.CAN-09-1451
24. Deng J, Wu Z, Zhao Z, et al. Berberine-loaded nanostructured lipid carriers enhance the treatment of ulcerative colitis. *Int j Nanomed*. 2020; Volume 15:3937–3951. doi:10.2147/IJN.S247406

25. Livak KJ, Schmittgen TD. Analysis of relative gene expression data using real-time quantitative PCR and the 2− ΔΔCT method. *methods*. 2001;25 (4):402–408. doi:10.1006/meth.2001.1262
26. Dong S, Lu Y, Peng G, et al. Furin inhibits epithelial cell injury and alleviates experimental colitis by activating the Nrf2-Gpx4 signaling pathway. *Digestive Liver Dis*. 2021;53(10):1276–1285. doi:10.1016/j.dld.2021.02.011
27. Xu L, Liu B, Huang L, et al. Probiotic consortia and their metabolites ameliorate the symptoms of inflammatory bowel diseases in a colitis mouse model. *Microbiol Spectr*. 2022;10(4):e00657–00622. doi:10.1128/spectrum.00657-22
28. Fujiki Y, Tanaka T, Yakabe K, et al. Hydrogen gas and the gut microbiota are potential biomarkers for the development of experimental colitis in mice. *Gut Microbiome*. 2024;5:1–24.
29. Liu G-H, Zhuo X-C, Huang Y-H, et al. Alterations in gut microbiota and upregulations of VPAC2 and intestinal tight junctions correlate with anti-inflammatory effects of electroacupuncture in colitis mice with sleep fragmentation. *Biology*. 2022;11(7):962. doi:10.3390/biology11070962
30. Tian M, Li D, Ma C, Feng Y, Hu X, Chen F. Barley leaf insoluble dietary fiber alleviated dextran sulfate sodium-induced mice colitis by modulating gut microbiota. *Nutrients*. 2021;13(3):846. doi:10.3390/nu13030846
31. Deng L, Zeng H, Hu X, et al. Se@Albumin nanoparticles ameliorate intestinal mucositis caused by cisplatin via gut microbiota-targeted regulation. *Nanoscale*. 2021;13(25):11250–11261. doi:10.1039/D0NR07981B
32. Zhou Y, Zhi F. Lower level of bacteroides in the gut microbiota is associated with inflammatory bowel disease: a meta-analysis. *Biomed Res Int*. 2016;2016:1–9. doi:10.1155/2016/5828959
33. Nguyen-Ngo C, Perkins AV, Lappas M. Selenium prevents inflammation in human placenta and adipose tissue in vitro: implications for metabolic diseases of pregnancy associated with inflammation. *Nutrients*. 2022;14(16):3286. doi:10.3390/nu14163286
34. Kalansuriya DM, Lim R, Lappas M. In vitro selenium supplementation suppresses key mediators involved in myometrial activation and rupture of fetal membranes. *Metallomics*. 2020;12(6):935–951. doi:10.1039/d0mt00063a
35. An J-K, Chung A-S, Churchill DG. Nontoxic levels of se-containing compounds increase survival by blocking oxidative and inflammatory stresses via signal pathways whereas high levels of se induce apoptosis. *Molecules*. 2023;28(13):5234. doi:10.3390/molecules28135234j